Role of Polymer–Salt–Solvent Interactions in the Electrospinning of Polyacrylonitrile/Iron Acetylacetonate

Jinmei Du, Xiangwu Zhang

Fiber and Polymer Science Program, Department of Textile Engineering, Chemistry, and Science, North Carolina State University, Raleigh, North Carolina 27695-8301

Received 21 December 2007; accepted 6 March 2008
DOI 10.1002/app.28396
Published online 20 May 2008 in Wiley InterScience (www.interscience.wiley.com).

ABSTRACT: Electrospinning is a process of producing ultrafine fibers by overcoming the surface tension of a polymer solution with electrostatic force. In this study, iron acetylacetonate was added to a polyacrylonitrile solution, and the role of polymer–salt–solvent interactions in the electrospinning of the ultrafine fibers was investigated. The polymer–salt–solvent interactions were characterized by Fourier transform infrared spectroscopy; and the solution viscosity, conductivity and surface tension were measured in solutions with different salt concentrations. The formation of polymer–salt–solvent interactions increased the solution viscosity, conductivity, and surface tension values at low salt concentrations. At high concentrations, the solution viscosity and surface tension decreased, but the conductivity remained relatively constant. The polymer–salt–solvent interactions influenced the structures of the electrospun fibers by changing the balance among the solution viscosity, conductivity, and surface tension. © 2008 Wiley Periodicals, Inc. J Appl Polym Sci 109: 2935–2941, 2008

Key words: association; composites; fibers; nanocomposites; nanotechnology

INTRODUCTION

Electrospinning is a relatively versatile, flexible, and easy method for producing ultrafine fibers with diameters ranging from 20 nm to 1 μm, and these fibers have a wide variety of applications, such as scaffolds for tissue engineering, filter media, protective clothing, capacitors, battery separators, and fuel cells.[1–5] Many polymers have been electrospun into ultrafine fibers, including polyacrylonitrile (PAN), polyethylene, polycarbonate, polystyrene, poly(vinyl alcohol), and collagen.[6,7] Among these polymers, PAN has been widely used to produce fine fibers because of the high dielectric constant that is desirable for electrospinning and many other applications.[8–10] PAN also provides well-known routes to carbon fibers, which can be used in many applications, such as sensors, catalyst supports, and batteries.[8] Compared with other polymer carbon precursors, PAN has advantages of a high carbon yield and flexibility in the control of the structure and properties of the final carbon fiber products.[11–13] In addition, salts are often added to the PAN precursors to obtain active carbon fibers.[14]

Many efforts have been carried out to study the electrospinning process, including studies on the effects of voltage, feed rate, and needle–collector distance.[15–17] However, there is less information in the literature about the role of polymer–salt–solvent interactions in the electrospinning of polymer fibers.[18] The addition of salts can introduce complicated polymer–salt–solvent interactions and can change solution properties, such as viscosity, conductivity, and surface tension.[19–22] The diameter of electrospun fibers is largely determined by the balance between the viscoelastic forces, electrostatic repulsion (conductivity), and surface tension.[23] Qin et al.[18] found that the addition of salts can change the viscosity of PAN solutions and the diameter of the resulting electrospun PAN. However, the influence of salt on other solution properties, such as conductivity and surface tension, was not addressed.

In this study, the polymer–salt–solvent interactions of PAN and iron acetylacetonate (AAI) solutions in *N*,*N*-dimethylformamide (DMF) were investigated. Their relationships to the solution properties, such as viscosity, conductivity, and surface tension, and the resultant fiber structure were established.

EXPERIMENTAL

Materials

AAI (purity = 99.9%), PAN (weight-average molecular weight = 150,000, typical), and DMF (purity = 99.8%) were purchased from Sigma-Aldrich (Milwaukee, WI). They were used without further purification.

Correspondence to: X. Zhang (xiangwu_zhang@ncsu.edu).

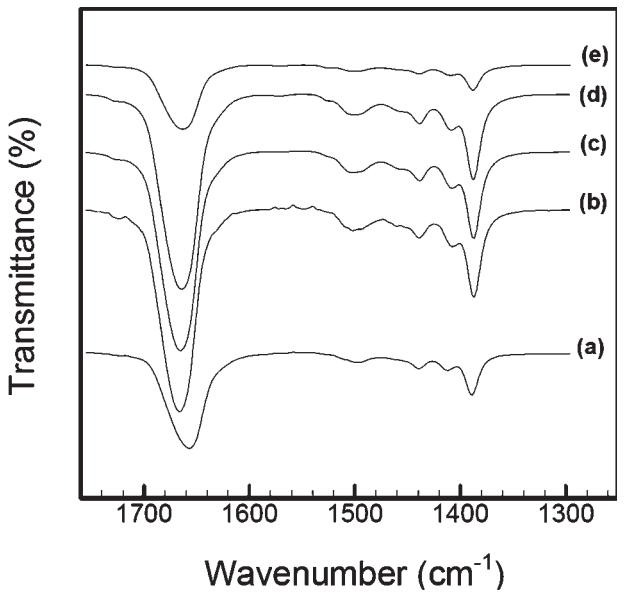

Figure 1 FTIR spectra of (a) DMF and the AAI + PAN + DMF solutions with different AAI concentrations: (b) 0, (c) 14, (d) 28, and (e) 57 μmol/g.

Solution preparation

Weighed PAN and AAI were added to DMF and stirred for 4 h; this was followed by ultrasonic vibration for 1 h. The PAN concentration in the solutions was 0.53 μmol/g (i.e., 8.0 wt %) and the AAI concentrations were 0, 8, 14, 23, 28, 42, and 57 μmol/g (i.e., 0, 0.3, 0.5, 0.8, 1.0, 1.5, and 2.0 wt %, respectively).

Electrospinning

The electrospinning was carried out by the application of a high voltage between the polymer solution contained in the syringe and the metallic collector. The dimensions of the needle were as follows: inner diameter = 0.012 in.; outer diameter = 0.022 in.; and length = 0.25 in. When the voltage reached a critical value, the electrostatic force overcame the surface tension of the solution and ejected a liquid jet, which was deposited on the collector in the form of ultrafine fibers. For all of the electrospinning experiments in this study, aluminum foil was placed on the collector for the deposition of fibers. The voltage used was 11.8 kV, the feed rate was 0.5 mL/h, and the needle–collector distance was 15 cm.

Characterization

The viscosity of the solutions was measured on a stress-controlled rheometer (ATS Rheosystems, Bordentown, NJ) with two 45-mm parallel plates at room temperature. The gap between the two plates was fixed at 0.300 mm. The surface tension of solutions was measured by a surface tensiomat tensiometer (Fisher Scientific, model 21, Pittsburgh, PA) at room temperature. Gamry reference 600 was used to obtain the conductivity of solutions. We assessed the reproducibility of the data by conducting all measurements on at least three samples.

A Nicolet Nexus (Ramsey, MN) 470 Fourier transform infrared (FTIR) spectrophotometer was used to record the FTIR spectra with a wave-number resolution of 0.5 cm^{-1}. The structure of the electrospun fibers was characterized by a Jeol 6400F field emission scanning electron microscope (SEM, Tokyo, Japan). The average fiber diameter was determined on the basis of the measurements of 50 randomly selected fibers in scanning electron microscopy images by Revolution v1.6.0b195 software.

RESULTS AND DISCUSSION

Polymer–salt–solvent interactions

To identify the interactions between PAN, AAI, and DMF, FTIR studies were carried out for the DMF solvent, PAN + DMF solution, and AAI + PAN + DMF solutions, and the results are shown in Figure 1. The major characteristic IR bands in DMF were ⟩C=O stretching (1656.9 cm^{-1}) and OC—N stretching (1389.1 cm^{-1}).[24] As also shown in Figure 1, the IR frequencies of ⟩C=O stretching and OC—N stretching changed after the addition of PAN and AAI into DMF. The observed band shifts for these two molecular motions in DMF are reported in Table I. After the addition of 0.53 μmol/g PAN into DMF, the ⟩C=O stretching shifted from 1656.9 to 1666.3 cm^{-1} and the OC—N stretching shifted from 1389.1 to 1387.2 cm^{-1}. These shifts were also found by Phadke et al.[19] and Padhye and Karandikar.[22] In general, there are two kinds of molecules in pure DMF, that is, free DMF molecules [Fig. 2(a)] and self-associated DMF molecules [Fig. 2(b)]. When PAN molecules are introduced into DMF, the relatively electronegative nitrogen of PAN interacts with electropositive nitrogen of OC—N of DMF, and a complex between the PAN and DMF molecules is formed [Fig. 2(c)], which causes the redshift (decrease in frequency) of OC—N stretching and the blueshift (increase in frequency) of ⟩C=O stretching.

TABLE I
Effects of PAN and AAI on the >C=O and OC—N Stretching Frequencies of DMF

	>C=O stretching (cm^{-1})	OC—N stretching (cm^{-1})
DMF	1656.9	1389.1
PAN + DMF	1666.3	1387.2
AAI (14 μmol/g) + PAN + DMF	1665.3	1387.4
AAI (28 μmol/g) + PAN + DMF	1664.2	1387.7
AAI (57 μmol/g) + PAN + DMF	1663.2	1388.0

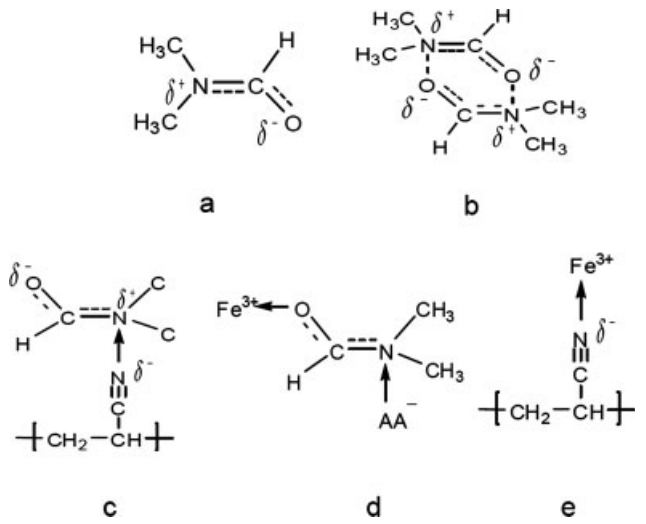

Figure 2 Depiction of the molecular structures and interactions among AAI, PAN, and DMF in solution.

As shown in Figure 1 and Table I, the addition of AAI into the PAN + DMF solution led to the redshift of the ⟩C=O stretching frequency at 1666.3 cm^{-1} and the blueshift of the OC—N stretching frequency at 1387.2 cm^{-1}. Both shifts became larger with increasing AAI concentration. These results indicate that DMF–salt and PAN–salt complexes were formed, and they reduced the amount of PAN–DMF complex in the solution. DMF–salt complexes formed because the electropositive nitrogen of DMF tends to interact with AA^-, which is more negative than the nitrogen in PAN [Fig. 2(d)]. The formation of PAN–salt complexes was due to the interaction between Fe^{3+} and the nitrogen in PAN [Fig. 2(e)]. Because DMF has a higher basicity than PAN,[25] the complex of DMF–salt was stronger than the PAN–salt complex, which indicated a larger intermolecular interaction in the DMF–salt than in the PAN–salt.

The formation of polymer–salt–solvent interactions had an impact on the solution properties, such as viscosity, conductivity, and surface tension, which in turn, affected the structure of the electrospun fibers.

Solution viscosity

Figure 3 shows the viscosity of the AAI + PAN + DMF solutions with different AAI concentrations. Up to an AAI concentration of 14 μmol/g (the number ratio of Fe^{3+} to the repeating unit of PAN was about 1:100), the solution viscosity increased with increasing AAI concentration. However, the viscosity decreased after the AAI concentration exceeded 14 μmol/g. The change in solution viscosity with AAI concentration was caused by the formation of PAN–salt and DMF–salt complexes in the AAI-added solutions. The ion Fe^{3+} is trivalent and has the potential to form complexes simultaneously with multiple oxygens in DMF and/or nitrogens in PAN and, hence, reduced the mobility of both PAN and DMF, which in turn, resulted in a higher solution viscosity. This effect was pronounced when the AAI concentration was low, and as a result, the solution viscosity increased with the addition of AAI when the AAI concentration was lower than 14 μmol/g. However, the formation of DMF–salt complexes also reduced the solvation power of DMF for PAN because fewer DMF molecules were available for interacting with PAN chains. In a poor solvent, the PAN chains would experience less coil expansion, that is, a lower viscosity. The effect of reduced DMF solvation power was more pronounced at high salt concentrations because the DMF solvation power was only significantly reduced after a large amount of DMF molecules formed complexes with AAI.[19] As a result, the solution viscosity decreased after the AAI concentration exceeded 14 μmol/g.

Solution viscosity has a significant influence on the morphology of electrospun fibers, and typically, increasing solution viscosity leads to an increase in the diameter of electrospun fibers[26,27] if other solution properties remain the same. However, the final fiber diameter is determined by the balance between the viscoelastic forces, electrostatic repulsion (conductivity), and surface tension, and hence, the solution conductivity and surface tension were also studied.[23]

Solution conductivity

Figure 4 shows the relationship between the solution conductivity and AAI concentration for the AAI +

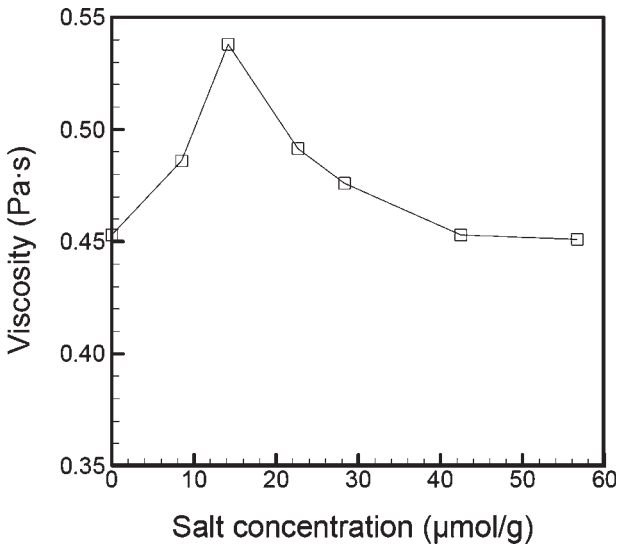

Figure 3 Relationship between the solution viscosity and AAI concentration of the AAI + PAN + DMF solutions.

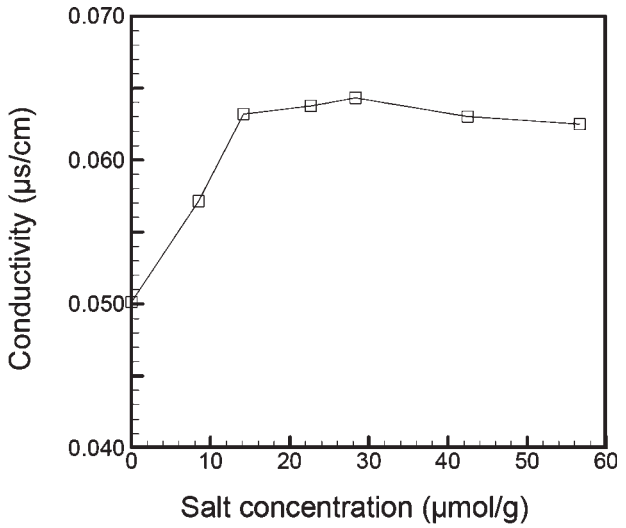

Figure 4 Relationship between the solution conductivity and AAI concentration of the AAI + PAN + DMF solutions.

PAN + DMF solutions. With increase in AAI concentration, the solution conductivity increased first and then remained relatively constant after AAI concentration exceeded 14 μmol/g. In general, the solution conductivity (σ) of a salt solution is governed by[28]

$$\sigma = \Sigma F z_j \mu_j c_j \quad (1)$$

where F is the Faraday constant and z_j, μ_j, and c_j are the charge, electrochemical mobility, and concentration of j, which is the type of ion. With the addition of AAI salts, more ions were introduced, which favored the increase of solution conductivity when the AAI concentration was lower than 14 μmol/g. However, as expected from eq. (1), the solution conductivity was also determined by the electrochemical mobility (or the drift velocity under the force exerted by the unit electric field on the ions), which decreased with increasing AAI concentration because of the formation DMF–salt and PAN–salt complexes. In addition, the charges in the solutions changed with the AAI concentration because charged ions may have formed electrically neutral ion pairs or charged ion aggregates; this is often found in solutions with high salt concentrations.[29] Therefore, the increase in AAI concentration had to compete with the changes in mobility and changes in ions, which was the reason the solution conductivity remained relatively constant at high AAI concentrations.

Solution surface tension

In addition to viscosity and conductivity, solution surface tension also plays an important role in the fiber formation. The surface tension is caused by the attractive force between the molecules on the surface of solution, with higher attractive forces leading to greater surface tension. Figure 5 shows the influence of the AAI concentration on the surface tension of the AAI + PAN + DMF solutions. The surface tension increased with the addition of AAI salt at AAI concentrations less than 28 μmol/g. After the AAI concentration exceeded 28 μmol/g, the solution surface tension decreased. The increase in the solution surface tension was caused by the formation of DMF–salt and PAN–salt interactions, which were stronger than the DMF–PAN and DMF–DMF interactions. However, at high AAI concentrations (>28 μmol/g), ions tended to form neutral ion pairs or charged ion aggregates,[29] which may have, in turn, led to weaker intermolecular interactions and a smaller surface tension.

Fiber structure

SEM images of the AAI+ PAN fibers electrospun from solutions with different salt concentrations are shown in Figure 6, and the average fiber diameters are shown in Figure 7. AAI concentration did not have a significant influence on the fiber surface structure; however, the fiber diameter varied slightly with AAI concentration. With increasing AAI concentration, the electrospun fiber diameter passed through a maximum. Typically, when the processing parameters (e.g., voltage, feed rate, and needle–collector distance) are fixed, the electrospinning process is mainly determined by the balance among the viscoelastic forces, electrostatic repulsion, and surface tension of the electrospinning solution. During electrospinning, the surface tension of a solution

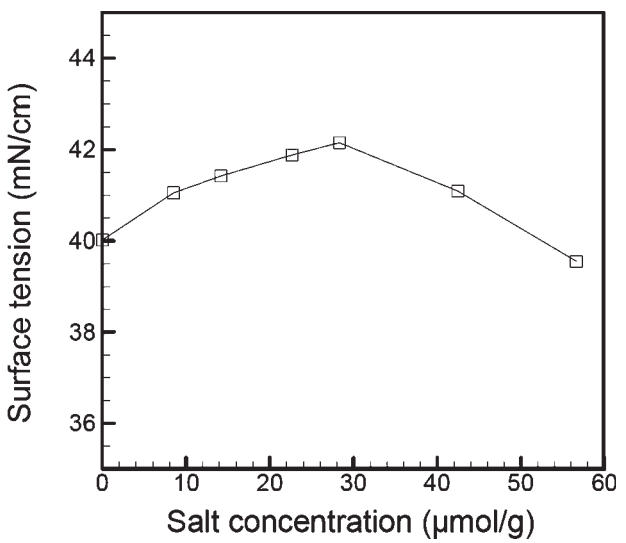

Figure 5 Relationship between the solution surface tension and AAI concentration of the AAI + PAN + DMF solutions.

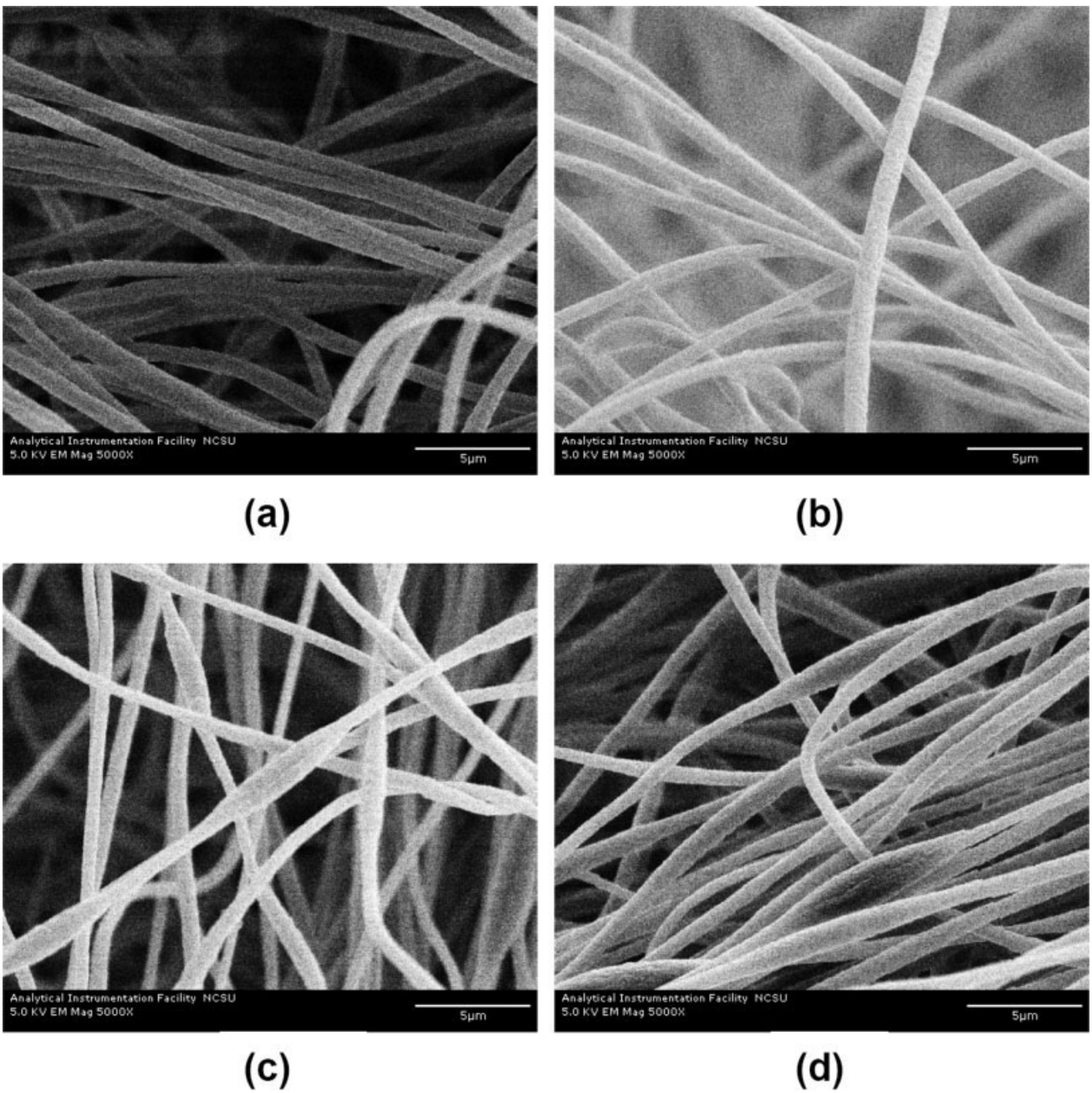

Figure 6 SEM micrographs of the electrospun fibers from the AAI + PAN + DMF solutions with different AAI concentrations: (a) 0, (b) 14, (c) 28, and (d) 57 μmol/g.

tends to keep the surface area of the jet to a minimum, which in turn, causes the formation of beads and spindles (even jet breakage in some cases). To obtain uniform fibers, the electrostatic repulsion must overcome the surface tension of the solution at the tip of the needle, and hence, a high solution conductivity is preferred during electrospinning. The solution viscosity should not be too low during electrospinning so that a steady jet can be obtained without being broken before it reaches the collector. However, the increase in solution viscosity also leads to the increased diameter of the electrospun fibers.[26,27]

In the AAI + PAN + DMF electrospinning solutions, the viscosity reached a maximum when the AAI concentration was 14 μmol/g, and at the same time, the solution conductivity reached a high value at this AAI concentration and remained relatively constant at higher AAI concentrations. However, the maximum surface tension was reached when the AAI concentration was 28 μmol/g. When the AAI concentration was 0, the surface tension of the solution was low, which favored the formation of smooth fibers [Fig. 6(a)]. The addition of 14 μmol/g AAI into the electrospinning solution increased the

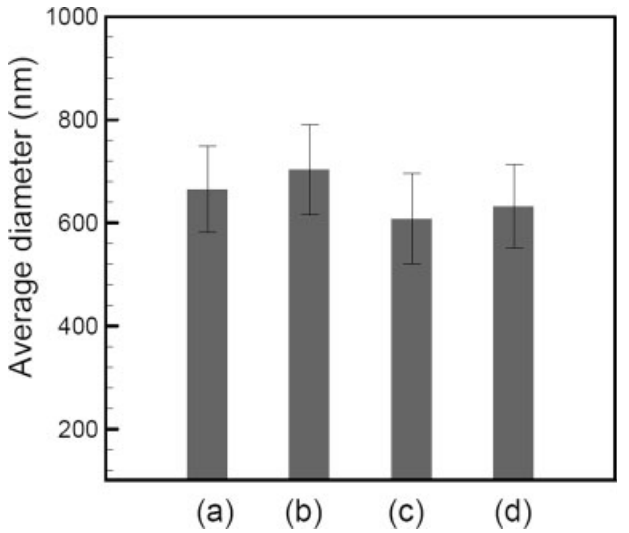

Figure 7 Average diameters of the fibers electrospun from the AAI + PAN + DMF solutions with different AAI concentrations: (a) 0, (b) 14, (c) 28, and (d) 57 μmol/g.

solution surface tension from 40.0 to 41.5 mN/m, which was detrimental to the formation of uniform fibers. However, the increases in the solution viscosity (from 0.45 to 0.54 Pa s) and conductivity (from 0.05 to 0.06 μs/cm) were sufficient to overcome the increase in surface tension, and hence, the resultant fibers were still uniform [Fig. 6(b)]. As shown in Figure 7, the fiber diameter increased from 665 to 705 nm at an AAI concentration of 14 μmol/g, which was mainly because of the increased viscosity.

As shown in Figure 7, when the AAI concentration was increased to 28 μmol/g, the fiber diameter decreased from 705 to 605 nm because the solution viscosity decreased from 0.54 to 0.48 Pa s. However, the solution surface tension continued to increase and reached a maximum of 42.0 mN/m, and at the same time, the solution conductivity remained relatively constant. As a result, spindles were formed in the electrospun fibers because of the increased surface tension [Fig. 6(c)]. At an AAI concentration of 57 μmol/g, both the solution viscosity and surface tension decreased, and the fiber structure did not change significantly [Fig. 6(d)].

CONCLUSIONS

The polymer–salt–solvent interactions of PAN and AAI solutions in DMF were investigated, and their relationships to the solution properties, such as viscosity, conductivity, and surface tension, and the resultant fiber structure were established. FTIR results indicate that a PAN–DMF complex was formed in the PAN + DMF solution, but the addition of AAI reduced the amount of PAN–DMF complex because of the formation of PAN–salt and DMF–salt complexes. The addition of AAI also increased the solution viscosity with a maximum value achieved at an AAI concentration of 14 μmol/g. The relationship between the solution surface tension and AAI concentration had the same trend with that between viscosity and AAI concentration, but the maximum surface tension was achieved at an AAI concentration of 28 μmol/g. Unlike the viscosity and surface tension, the solution conductivity first increased with increasing AAI concentration and then remained relatively constant after the AAI concentration exceeded 14 μmol/g.

The changes in solution viscosity, conductivity, and surface tension had an influence on the electrospun fiber structure. With increasing AAI concentration, the electrospun fiber diameter first increased because of the increased solution viscosity but passed through a maximum at an AAI concentration of 14 μmol/g. In addition, at low AAI concentrations ($\leq$14 μmol/g), the solution viscosity and conductivity were sufficient to overcome the surface tension, and hence, the electrospun fibers were uniform. However, spindles were formed at an AAI concentration of 28 μmol/g because of the increased surface tension.

The authors thank Wendy Krause for useful suggestions and all of the other friends who gave us help during this research.

References

1. Ma, Z. W.; Kotaki, P.; Ramakrishna, S. J Membr Sci 2005, 265, 115.
2. Podgorski, A.; Balazy, A.; Gradon, L. Chem Eng Sci 2006, 61, 6804.
3. Bessel, C. A.; Laubernds, K.; Rodriguez, N. M.; Baker, R. T. K. J Phys Chem B 2001, 105, 1115.
4. Steigerwalt, E. S.; Deluga, G. A.; Cliffel, E. D.; Lukehart, C. M. J Phys Chem B 2001, 105, 8097.
5. Yuan, F. L.; Sasikumar, G.; Ryu, H. J. New Mater Electr Sys 2004, 7, 311.
6. Givens, S. R.; Cardner, K. H.; Rabolt, J. F.; Chase, D. B. Macromolecules 2007, 40, 608.
7. Wang, C.; Hsu, C. H.; Lin, J. H. Macromolecules. 2006, 39, 7662.
8. Zhang, X. W.; Wang, Y. Z.; Sun, C. F. J Polym Res 2007, 14, 467.
9. Wang, C.; Chien, H. S.; Hsu, C. H.; Wang, Y. C.; Wang, C. T.; Lu, H. A. Macromolecules 2007, 40, 7973.
10. Cho, T. H.; Sakai, T.; Tanase, S.; Kimura, K.; Kondo, Y.; Tarao, T.; Tanaka, M. Electrochem Solid State Lett 2007, 10, A159.
11. Kim, C.; Yang, K. S.; Kojima, M.; Yoshida, K.; Kim, Y. J.; Kim, Y. A.; Endo, M. Adv Funct Mater 2006, 16, 2393.
12. Sreekumar, T. V.; Liu, T.; Min, B. G.; Guo, H.; Kumar, S.; Hauge, R. H.; Smalley, R. E. Adv Mater 2004, 16, 58.
13. Sutasinpromprae, J.; Jitjaicham, S.; Nithitanakul, M.; Meechaisue, C.; Supaphol, P. Polym Int 2006, 55, 825.
14. Oya, A.; Yoshida, S.; Alcanizmonge, J.; Linaressolano, A. Carbon 1995, 33, 1085.

15. Li, D.; Xia, Y. Adv Mater 2004, 16, 1151.
16. Zhang, Y. Z.; Wang, X.; Feng, Y.; Li, J.; Lim, C. T.; Ramakrishna, S. Biomacromolecules 2006, 7, 1049.
17. Fong, H.; Chun, I.; Reneker, D. H. Polymer 1999, 40, 4585.
18. Qin, X. H.; Yang, E. L.; Li, N.; Wang, S. Y. J Appl Polym Sci 2007, 103, 3865.
19. Phadke, M. A.; Musale, D. A.; Kulkarni, S. S.; Karode, S. K. J Polym Sci Part B: Polym Phys 2005, 43, 2061.
20. Qin, X. H.; Yang, E. L.; Li, N.; Wang, S. Y. J Appl Polym Sci 2007, 103, 3865.
21. Lee, H. J.; Won, J.; Lee, H.; Kang, Y. S. J Membr Sci 2002, 196, 267.
22. Padhye, M. R.; Karandikar, A. V. J Appl Polym Sci 1985, 30, 667.
23. Fridrikh, S. V.; Yu, J. H.; Brenner, M. P.; Rutledge, G. C. Phys Rev Lett 2003, 90, 144502.
24. Jacob, M. M. E.; Arof, A. K. Electrochim Acta 2000, 45, 1701.
25. Gutmann, V.; Resch, G.; Linert, W. Coord Chem Rev 1982, 43(May), 133.
26. Fong, H.; Chun, I.; Reneker, D. H. Polymer 1999, 40, 4585.
27. Mckee, M. G.; Wilkes, G. L.; Colby, R. H.; Long, T. E. Macromolecules 2004, 37, 1760.
28. Bohnke, O.; Frand, G.; Rezrazi, M.; Rousselot, C.; Truche, C. Solid State Ionics 1993, 66, 105.
29. Bruce, P. G. Synth Met 1991, 45, 267.